

GHGT-11

Flue gas injection for CO₂ storage and enhanced coalbed methane recovery: Mixed gas sorption and swelling characteristics of coals

Amer Syed*, Sevket Durucan, Ji-Quan Shi, Anna Korre

Department of Earth Science and Engineering, Royal School of Mines, Imperial College London, London SW7 2BP, UK

Abstract

The impact of coal pore structure on adsorption-induced matrix swelling of three coals of different ranks was investigated experimentally. The swelling strain measurements for the selected samples of the two higher rank coals suggested that variation in the sample pore size distribution, particularly the microporosity, has a larger impact on matrix swelling induced by adsorption of CO₂ than by adsorption of less adsorbing gases. The swelling behaviour recorded for the low rank coal may be explained by the level of microporosity or lack of it. From flue gas ECBM point of view, the swelling strain data tentatively suggests that the low rank coal would experience less swelling, compared to the higher rank coals.

© 2013 The Authors. Published by Elsevier Ltd.
Selection and/or peer-review under responsibility of GHGT

Keywords: Coal pore structure; microporosity; flue gas sorption; matrix swelling; ECBM

1. Introduction

Coal is characterised as a dual porosity reservoir rock system, which consists of porous-solid blocks known as matrix (primary porosity), bounded by a well-defined network of natural fractures known as cleats (secondary porosity). The cleats are the main flow conduits in a coal seam, whereas methane is primarily stored by adsorption in the micropores (pore size < 2 nm) of the coal matrix. Current commercial production of Coalbed Methane (CBM) is primarily through pressure depletion in the reservoir. Enhanced recovery, involving injecting CO₂ or N₂, has long been proposed as a potentially viable means to improve

* Corresponding author. Tel.: +44-20-7594-7374; fax: +44-20-7594-7444.
E-mail address: shafiuddinamer.syed07@imperial.ac.uk

CBM recovery [1]. Using CO₂ for Enhanced Coalbed Methane (ECBM) recovery is attractive as it has the added advantage of storing CO₂ in deep coal seams. However, adsorption of CO₂ in coal causes it to swell, which has a severe detrimental impact on its permeability. To overcome CO₂ adsorption induced permeability reduction, Durucan and Shi [2] investigated the injection of a binary mixture of N₂ and CO₂ using horizontal wells. In a micro-pilot [3] involving injection of flue gas (87.5% N₂ and 12.5% CO₂) in Alberta, Canada, increase in injectivity was reported. If this technology is to be implemented at larger scales, a better understanding of the physics of mixed gas adsorption on coal and the associated swelling is required.

The aim of the work presented here is to assess the effect of coal pore size distribution, especially the microporosity, on matrix swelling induced by adsorption of flue gas (87% N₂ and 13% CO₂), as well as pure gases, and the implication for flue gas ECBM.

2. Experimental procedure

Three coal types of different ranks (designated as Coal A, Coal B and Coal C) from the Scottish coalfields were selected. The proximate analysis results for the three coals are given in Table 1.

Table 1. Characteristics of coals used in the study

	Coal A	Coal B	Coal C
Fixed Carbon (d.a.f) (%)	85.55	72.41	60.90
Volatile Matter (d.a.f) (%)	15.45	27.59	39.10
Rank, UK (American)	Coking steam (Low volatile bituminous)	Medium volatile coking (Medium volatile bituminous)	High volatile (High volatile bituminous B/A)
Total porosity (fraction)	0.02-0.04	0.04-0.1	0.04-0.06

These coal samples were retrieved as 150 mm diameter cores from exploration wells and were transported to the laboratory immersed in water to retain moisture and prevent damage. Once received the coal samples were stored in a desiccator at constant humidity and temperature. Sample cubes were cut from these samples and prepared for the experimental work. Prior to their use, the coal samples were subjected to vacuum in a Pyrex© brand large diameter vacuum desiccator supplied by Fischer Scientific UK, were flooded with distilled water for more than 48 hours[4].

2.1. Pore size distribution

In this study solid state H¹ Nuclear Magnetic Resonance (H¹ NMR) logs were used to characterise the pore size distribution of the coal samples. A distinct advantage of this technique is the ability to capture the entire pore size distribution ranging from submicropores to cleats; and the non-destructive nature of the process facilitates the use of the same sample for further analysis. H¹ NMR is based on the relaxation behaviour of proton in the pore fluid of the rock when subjected to an external magnetic field. The transverse relaxation time (T_2) of the protons in the pore fluid is widely used in the petroleum industry to map the hydrocarbons and to estimate the porosity of the subsurface formations [5]. The signal amplitude distribution of transverse relaxation time T_2 extracted from the NMR logs is an indicator of the pore size distribution of the coal sample [6]. Although it is not possible to translate the NMR observations directly into pore size as the surface relaxivity of the fluid rock system is not quantitatively known, it is possible to correlate and compare the pore volumes for various coal samples.

NMR measurements were carried out at a temperature of 34°C using a 2 MHz, 0.5T, MARAN Instrument supplied by Oxford Instruments (UK). A CPMG [7, 8] pulse sequence was used to produce a closely spaced echo train with interecho time of 200 μ s and 8000 of those echos were captured for each of the 300 scans. The amplitudes of the resulting echo trains were fitted with a multimodal Distributed Exponential Fit (DXP) [6] and were plotted against the logarithmic T_2 value in microseconds. For comparison, a surface relaxivity of 0.66 nm/ms was assumed. Following IUPAC classification: the T_2 relaxation <0.2 ms corresponds to sub-micropores (pore size<0.8 nm); 0.2< T_2 <1ms represents micropores (0.8 nm<pore size<2 nm); 1< T_2 <25 ms indicates mesopores (2 nm <pore size<50 nm); and T_2 >25 ms yields macropores (pore size>50 nm).

2.2. Adsorption of pure and mixed gases

The experimental setup used for adsorption isotherm measurements is based on Boyle's law (Fig. 1). It consists of a stainless steel cylindrical sample cell in which crushed coal sample can be introduced. The sample cell is connected to a reference volume through steel tubing of diameter 3.17 mm. An expansion valve connects the sample cell to the reference cell and the pressure is monitored through a transducer sourced from Druck UK Ltd.

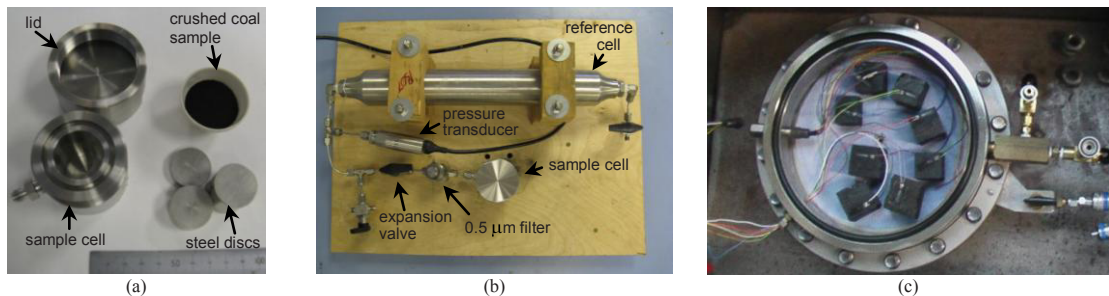


Fig. 1. (a) and (b) Experimental set up for adsorption isotherm ; (c) matrix swelling measurements.

An inline filter of size 0.5 micron, supplied by Swagelok UK, is placed before the sample cell to prevent the migration of coal fines into the tubings and reference cell. The setup is enclosed in a temperature controlled Hereaus 300 litre oven, supplied by Thermo Fischer GmbH, Germany, operating within 0.2 °C. The sample for the tests is prepared by crushing the coal sample and sieving to extract particles of uniform grain size of 150 μ m. All the experiments were conducted for dry coal at constant temperature of 26 °C.

2.3. Sorption induced matrix swelling

Approximately 25 mm cubes (or rectangular prisms) of coal samples, with machine-smoothed surfaces mutually perpendicular to each other were used for matrix swelling experiments. High precision strain gauges were pasted on the mutually perpendicular directions on the coal sample. The samples were loaded into a 10 MPa high pressure moisture extractor cell (Figure 1c), which in turn was enclosed in an oven to maintain constant temperature throughout the experiments. The strain gauge leads from the cell were connected to an automatic data logging system which was connected to a desktop computer to record strain measurement data. Gas was injected into the cell in pressure steps of 0.5 MPa and the pressure in the cell was maintained during each step. The strain readings were monitored and, once the strains are stabilised, the pressure of the gas in the cell was increased to the next pressure step. The time

required to reach equilibrium and stabilisation of the strains depended on the gas injected, adsorption rate/volume and gas pressure.

3. Results and discussion

3.1. Pore size distribution

The T_2 measurement and the inferred pore size distribution of selected samples for each coal type is shown in Fig. 2. It can be seen that Coal A (low volatile bituminous) and Coal B (medium volatile bituminous) generally exhibit bi-modal pore structure, with pore volume mainly residing in micro-/meso- and macropores. It is noted Coal B is largely dominated by macroporosity. This is consistent with visual inspection of the samples, which shows significant cleats in all the samples. On the other hand, pore volume in the four Coal C (high volatile bituminous) samples tested was concentrated in a rather narrow range, varying from micropore (C3 and C4) to macropore (C1). No signal was recorded for sample C2. Visual observation of the Coal C samples revealed pyrite depositions and a rough and dull texture.

From the pore size distribution of the coal samples tested, the microporosity fraction for each coal type may be estimated. This ranges from 0.33 to 0.54 for Coal A, 0.17 to 0.53 for Coal B and 0 to 1 for Coal C. As coal A is relatively higher rank with fixed carbon around 80%, the presence of large microporosity is expected. Similar observation on higher microporosity for bright coals was also reported in the literature [10].

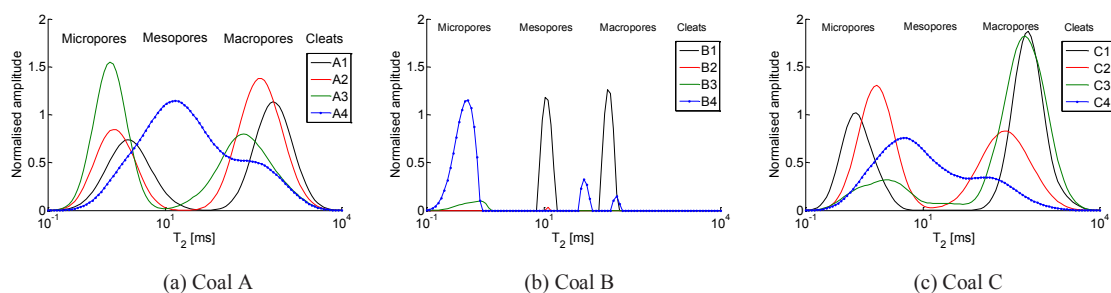


Fig. 2. NMR pore size distribution of the samples for the three coal types (solid line – Sample 1; red line – Sample 2; green line – Sample 3; solid blue with symbol – Sample 4).

3.2. Pure and mixed gas adsorption

Sorption isotherms for N_2 , CH_4 , and flue gas (13% CO_2 /87% N_2) and CO_2 were measured on crushed samples of the three coals at a controlled temperature of 26 °C. For each coal, the test was repeated on different batch of samples. The sorption measurements were found to be very consistent. As shown in Figure 3, the sorption data (excess adsorption) for N_2 , CH_4 and CO_2 for the three coals can be fitted well with Langmuir equation, $V = V_L p / (P_L + p)$. The fitted parameters, namely Langmuir volume V_L and Langmuir pressure P_L , are listed in Table 2. As would be expected, CO_2 has the highest sorption affinity, followed by CH_4 , and then N_2 . Figure 4 compares the measured sorption isotherms for the three coals. It can be seen that the lowest rank Coal C has the least sorption capacity among the three coals, as would be expected.

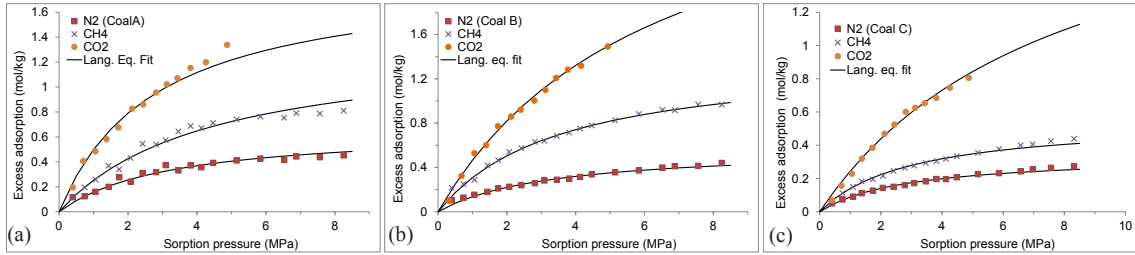


Fig. 3. Measured excess adsorption and fitted Langmuir isotherm curves for pure gases for the three coals.

Table 2. Fitting Langmuir equation to the sorption data for the three coals – Langmuir volume and pressure.

	N ₂		CH ₄		CO ₂		Flue gas	
	V _L	P _L	V _L	P _L	V _L	P _L	V _L	P _L
	mol/kg	MPa	mol/kg	MPa	mol/kg	MPa	mol/kg	MPa
Coal A	0.67	3.23	1.36	4.37	1.90	2.81	2.27	8.41
Coal B	0.58	3.30	1.39	3.53	3.42	6.35	2.78	8.13
Coal C	0.34	2.85	0.55	2.97	2.18	7.94	1.57	6.89

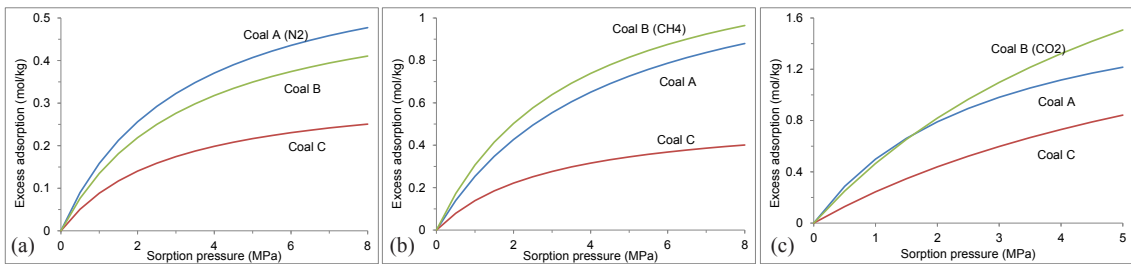


Fig. 4. Comparison of sorption isotherms among the three coals.

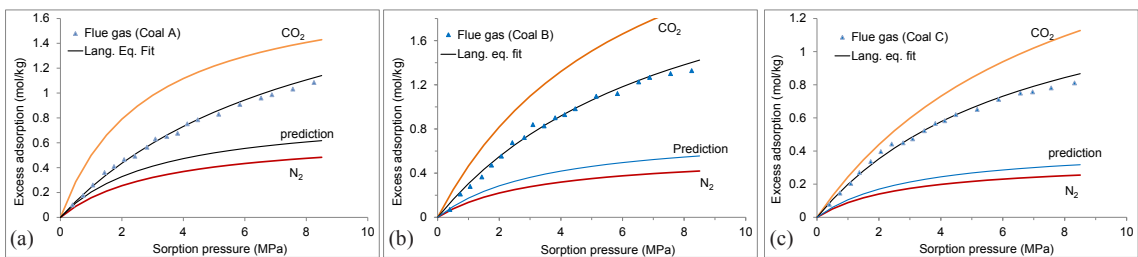


Fig. 5. Flue gas isotherms and Langmuir equation fit for the three coals.

Based on the fitted Langmuir parameters for N₂ and CO₂, an attempt was made to fit the flue gas sorption data using the extended Langmuir equation. It was found that the prediction based on the known parameters for the pure gas components would considerably underestimate flue gas adsorption for all three coals (Fig. 5). Indeed, the flue gas data, despite its low CO₂ content, are seen to lie closer to those

for CO₂, rather than N₂. It would seem that CO₂ component has a much more pronounced influence on the sorption behaviour of the mixed gas than given by the extended Langmuir equation. The Langmuir parameters use are given in Table 2 (last column).

3.3. Sorption induced matrix swelling

Matrix swelling caused by adsorption of the pure gases (N₂, CH₄ and CO₂) and flue gas were measured for the selected samples of each coal. The results are presented in Figure 6 for the pure gases and Fig. 7 for the flue gas. For Coal A (Fig. 6a-c) and Coal B (Fig. 6d-f, the measured swelling strains for N₂ and CH₄ for the individual samples, except for A4, are relatively consistent with each other. In comparison, the sample data are more scattered for CO₂ for both coals. On the other hand, swelling strain was measured in only two of the samples (C3 and C4) for Coal C, which have predominantly microporosity; and the swelling for C4, with a larger microporosity, is consistently higher than C3. In addition, the strain measurement for N₂ is dominated by matrix compression (negative) for all the Coal C samples, as reflected in the consistency of the data and the almost perfect linear relationship between strain and gas pressure ($\epsilon = -71.5p$).

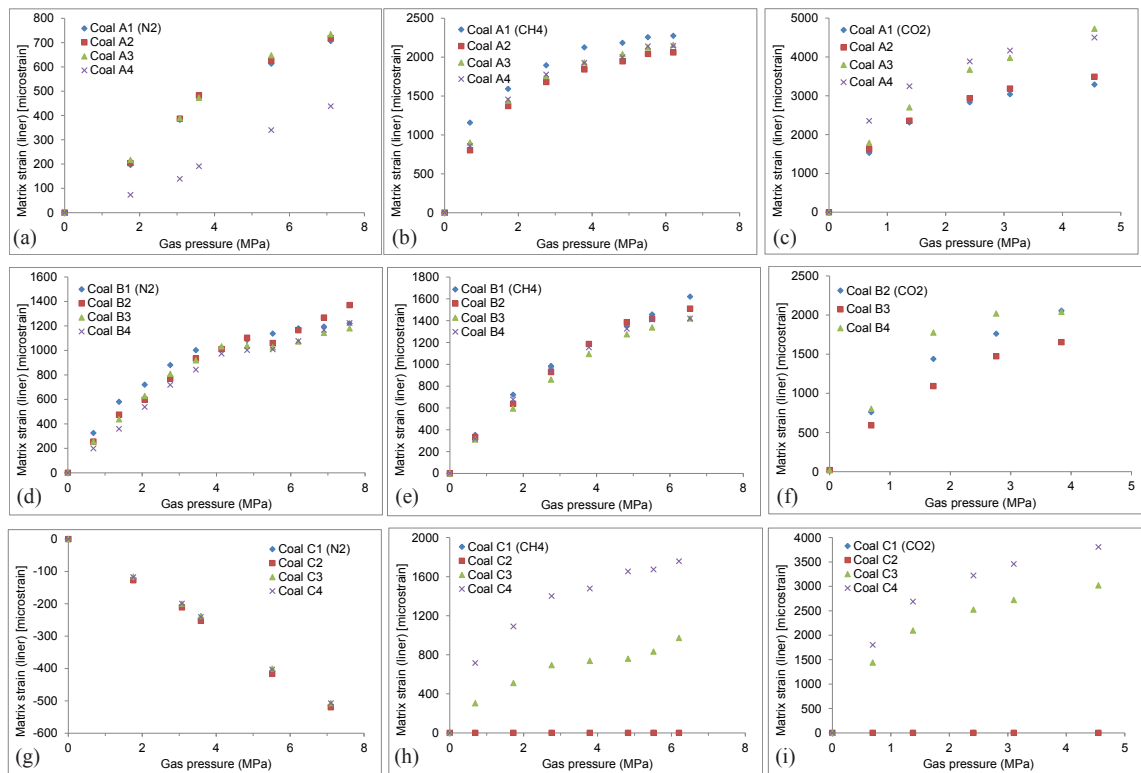


Fig. 6. Measured swelling strain for the pure gases for the selected samples of the three coals.

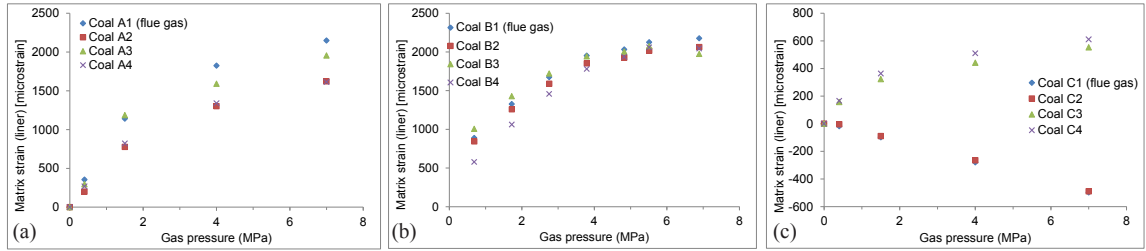


Fig. 7. Measured swelling strain for the flue gas for the selected samples of the three coals

Coal matrix swelling strain is made up of two parts: strain gauge reading and compressive mechanical strain due to the cell gas pressure (see Fig. 6g). In this study, the compressive strain at a given gas pressure was estimated using the relationship obtained above for Coal C. Thus swelling strain can be calculated for each coal sample tested. For ease of analysis, the sample-average value was used for the three coals. The swelling strains thus obtained for the pure gases were fitted with Langmuir type equation $\epsilon_s = \epsilon_L p / (P_\epsilon + p)$. The fitted curves, together with the standard deviation, are plotted in Fig. 8, with the fitted parameters (ϵ_s , P_ϵ) listed in Table 3. It is noted that the swelling strains for the three coals do not necessarily follow their rank in sorption capacity (Fig. 4). In particular, although Coal C has the lowest sorption capacity, its CH₄ swelling strain is comparable to that of Coal B (Fig. 8b) and considerably higher for CO₂, approaching to that of coal A (Fig. 8c).

As for flue gas adsorption, the flue gas swelling strain could also be fitted well with the Langmuir type equation. The fitted curves and the parameters are respectively presented in Fig. 9a and Table 3 (last column). For cross reference, the fitted flue gas sorption isotherms are also shown (Fig. 9b). The ratio of these two, which gives an indication of swelling strain per unit volume of adsorbed gas, is plotted in Fig. 9c. It can be seen that Coal C has the least tendency to swell (lowest swelling strain per unit adsorbed volume). Interestingly the two higher rank coals have comparable, though varying, ratios.

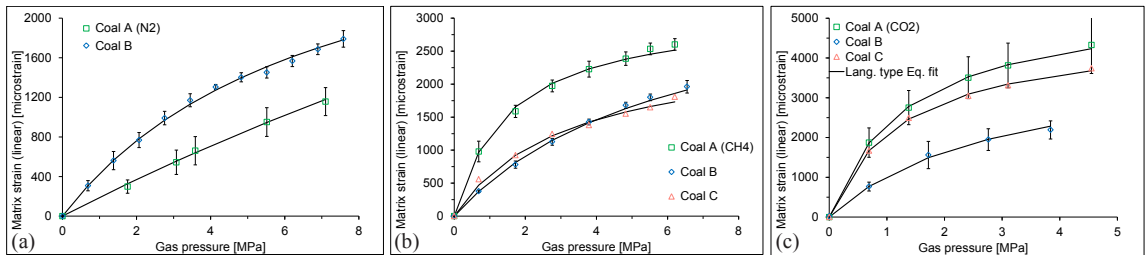


Fig. 8. Sample-averaged sorption induced swelling strain measurement and Langmuir-type equation fit.

Table 3. Fitting Langmuir-type equation to the swelling data for the three coals – Langmuir swelling strain and swelling pressure.

	N ₂		CH ₄		CO ₂		Flue gas	
	ϵ_L microstrain	P_ϵ MPa	ϵ_L microstrain	P_ϵ MPa	ϵ_L microstrain	P_ϵ MPa	ϵ_L microstrain	P_ϵ MPa
Coal A	8292	42.8	3141	1.54	5479	1.34	3228	2.96
Coal B	3419	6.97	3698	6.11	4012	2.90	3095	1.78
Coal C	-	-	2608	3.14	4683	1.24	1561	3.73

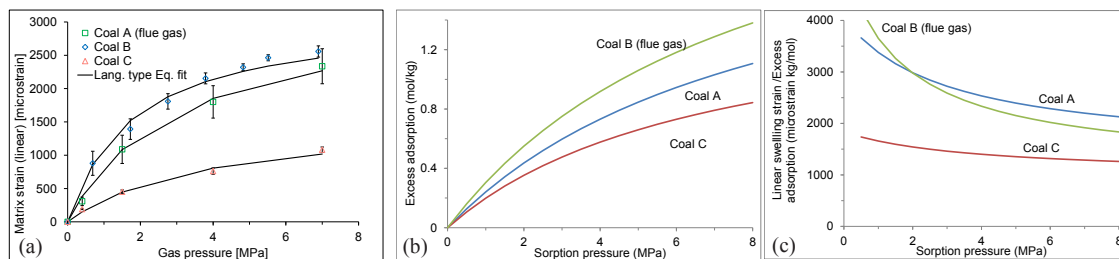


Fig. 9. Flue gas swelling strain and its correlation with sorption for the three coals.

4. Conclusions

Research has shown that the predicted sorption isotherms for the flue gas using the extended Langmuir equation and the parameters for the pure gas components (N_2 and CO_2) were found to be significantly lower compared to the test data.

The NMR test results showed that the two higher rank coals (Coal A and Coal B) generally exhibit bimodal pore structure, whereas the pore structure of the low rank Coal C is highly variable, with the pore volume residing in a rather narrow range of pore size, varying from micropores to macropores. The swelling strain measurements for the selected samples of the two higher rank coals suggested that variation in the sample pore size distribution, particularly the microporosity, has a larger impact on matrix swelling induced by adsorption of CO_2 than by adsorption of less adsorbing gases. The swelling behaviour recorded for Coal C samples may be explained by the level of microporosity or lack of it (C1).

From flue gas ECBM point of view, the swelling strain data tentatively suggests that the low rank coal C would experience less swelling compared to the higher rank coals.

Acknowledgements

The authors wish to thank Composite Energy Ltd., the BG Group, Scottish Power and the Royal Bank of Scotland for their support and funding of the research reported in this paper.

References

- [1] Puri R, Yee D. Enhanced coalbed methane recovery., *SPE* 1990;20732-MS:193-201.
- [2] Durucan S, Shi JQ. Improving the CO_2 well injectivity and enhanced coalbed methane production performance in coal seams. *International Journal of Coal Geology* 2009;77:214-21.
- [3] Mavor MJ, Gunter WD, Robinson JR. Alberta multiwell micro-pilot testing for CBM properties, enhanced recovery and CO_2 storage potential. *SPE Annual Technical Conference and Exhibition* 2004; 90256.
- [4] Dabbous MK, Reznik AA, Taber JJ, Fulton PF. The permeability of coal to gas and water. *SPE Journal* 1974;14(9):563-72.
- [5] Kenyon WE. Nuclear magnetic resonance as a petrophysical measurement. *Int. J. Radiation Appl. Inst. Part E. Nuclear Geophysics* 1992;6(2):153-71.
- [6] Coates GR, Xia L, Prammer MG. *NMR Logging- Principles and Applications*. Houston: Halliburton; 1999.
- [7] Carr HY Purcell EM. Effects of diffusion on free precession in nuclear magnetic resonance experiments. *Physical Review* 1954;94:630-38.
- [8] Meiboom S, Gill D. Modified spin echo method for measuring nuclear relaxation times. *Review of Scientific Instruments* 1958; 29:688-91.
- [9] IUPAC. Recommendations for the characterization of porous solids, *Pure and Applied Chemistry* 1994:1739-58.
- [10] Clarkson CR, Bustin RM. The effect of pore structure and gas pressure upon the transport properties of coal: a laboratory and modeling study: 1. Isotherms and pore volume distributions. *Fuel* 1999;78(11):1333-44.